eJNDT e-Journal of Nondestructive Testing - ISSN 1435-4934 - www.ndt.net

EWSHM 2024
11th European Workshop on Structural Health Monitoring

Physics-Informed Machine Learning for Structural Damage Diagnosis in Aluminium Plates

Lucio PINELLO[1], Luca LOMAZZI[1], Jacopo GHELLERO[1], Marco GIGLIO[1], Francesco CADINI[1]
[1] Department of Mechanical Engineering, Politecnico di Milano, Milan, 20156, Italy, e-mail:
lucio.pinello@polimi.it luca.lomazzi@polimi.it jacopo.ghellero@polimi.it
marco.giglio@polimi.it francesco.cadini@polimi.it

Abstract. Damage diagnosis plays a crucial role in Structural Health Monitoring (SHM) by facilitating the identification, localization, and estimation of the extent of defects in structures. Lamb waves, known for their sensitivity to defects, are widely employed in SHM methods for thin-walled structures. Most of those traditional methods require extracting damage indices from Lamb wave signals. This operation involves substantial post-processing and implies that part of the diagnostic information is lost. To solve those limitations and improve the damage diagnosis accuracy, machine learning methods have recently been proposed in the literature. However, the reluctance of the industrial sector to adopt conventional black-box models due to their lack of explainability poses a challenge.

This study proposes a physics-informed machine-learning approach to address the limitations of standard black-box methods. Particularly, a Physics-Informed Neural Network (PINN) is implemented to predict the density of an aluminium plate based on measurements of plate displacements caused by Lamb wave excitation. This is made possible by the implementation of a specific loss function, which leverages physical knowledge in the form of the partial differential equation governing Lamb waves.

Predicting the plate density based on measured displacements eliminates the need for artificial damage indices, utilizing the density variation itself to detect and localize damage. Additionally, the outputs of the PINN, rooted in physics equations, offer enhanced explainability compared to standard black-box models. The versatility of this framework extends to predicting material properties distributions for components, and efforts will be directed towards adapting the method for composite materials, where the approach may pose additional challenges.

Keywords: corrosion monitoring, SHM, transfer learning, neural network

https://doi.org/10.58286/29742

Introduction

Structural Health Monitoring (SHM) is a monitoring strategy that relies on a sensor network permanently installed on the structure or component of interest to allow its continuous monitoring, significantly reducing the time between two consecutive inspections. Among the several non-destructive techniques (NDT) used in the SHM framework, ultrasonic-guided waves, and in particular the Lamb waves, proved to be effective for thin-walled structures [1] [2] [3] [4] by exploiting a piezoelectric (PZT) sensor network for both wave excitation and reception. Focusing on Lamb waves, they have been extensively used for imaging and tomographic methods [5] [6] [7]. However, these methods require the extraction of features from the signals to obtain damage indexes (DIs) [1] [8] [9]. Similarly, machine learning (ML) algorithms are being applied due to the necessity of having real-time, or almost real-time, performance for SHM purposes. However, conventional ML approaches often are supervised methods and do not solve the need for a pre-processing phase to extract damage features from signals [10] [11] [12].

Therefore, there is a need for alternatives belonging to the unsupervised framework scheme. It is in this framework that Physics-Informed Neural Networks (PINNs) are gaining growing interest. This class of algorithm combine the information about the system physics, thanks to analytical models, with the neural networks' capacity to learn from the data. This is achieved by implementing tailored loss functions based on the Partial Differential Equations (PDEs) describing the phenomenon of interest [13] [14] [15] [16].

In this work, a PINN-based framework is developed focusing on the estimation of the material properties relying on Lamb waves signals measured through a PZT sensor network avoiding any pre-processing and DIs extraction phase. In the literature, but outside the SHM framework, two approaches are proposed for acoustic wave reconstruction (e.g., displacement field reconstruction) and inversion (e.g., material properties estimation given the displacement field); (i) the first relies on two neural networks trained together, one for material distribution prediction and the other for reconstructing the displacement field [17], while (ii) the second approach exploits a finite difference solver to predict the displacements, exploiting only a neural network for the estimation of material properties [18].

Therefore, in this work, the two approaches have been tested and compared for damage localisation simulating Lamb wave excitations for SHM purposes. Initially, the methods are compared for a 1D non-homogeneous clamped-clamped string. Then, the second approach was tested to perform damage localisation in a 2D domain represented by a plate section subjected to plain strain and constrained with clamps at both ends. In both case studies, the wave is a symmetric mode Lamb wave, as commonly used in the SHM field, and is excited in the middle of the domain with a tone burst.

1. Methodology

1.1 Theoretical Background

Lamb waves refer to ultrasonic-guided waves that move through slender structures like plates and shells. In contrast to bulk waves, Lamb waves are restricted to the structure's thickness. This confinement enables them to engage with defects, boundaries, and other features within the material. This characteristic enhances their effectiveness in identifying flaws in various engineering components, such as aircraft wings, pipelines, and bridges. Lamb waves' behaviour can be described by Eq. 1

$$\rho u_{tt} = \nabla \cdot (\sigma) + f \quad (1)$$

where ρ is the density, f is the forcing vector, u_{tt} is the second derivative of the displacement with respect to the time variable t, and $\nabla \cdot$ is the divergence operator applied to stress tensor σ. The stress tensor hinders the material properties through the constitutive relationship for elastic material by linking the Young's modulus E and the Poisson ratio ν with the displacement vector u. Eq. 1 can be used to describe Lamb wave propagation in one-dimensional, two-dimensional, and three-dimensional domains. For the sake of simplicity, only the theoretical steps for the mono-dimensional wave equation are described in this work, which represents an axial wave that propagates along the x coordinate through a one-dimensional string with the two ends fully constrained, e.g., clamped.

The introduction of variable material properties, essential for representing real scenarios such as damages and holes within the components, can be achieved by making explicit the constitutive law for elastic materials in Eq. 1. This allows the definition of the wave speed $c(x)$ as in Eq. 2, where the wave speed is a function of the x location on the string. For the sake of simplicity, the variable wave speed can be considered as the product of a constant term c_0, that is defined by the ratio between Young's modulus E and density ρ, with a variable parameter $\gamma(x)$ that is a function of the position on the string. The parameter $\gamma(x)$ lies in the domain $[0; 1]$ and, therefore, is representative of the actual distribution of the material properties along the domain. For instance, if there are no flaws, the actual value of the material properties should be equal to the nominal one ($\gamma = 1$ for every point in the domain) while cracks or any damage will reduce the stiffness of the material, leading to $\gamma < 1$ where the damage is present.

$$\mathrm{c(x)}^2 = \gamma(\mathrm{x})\mathrm{c}_0^2 = \gamma(\mathrm{x})\frac{\mathrm{E}}{\rho} \quad (2)$$

Therefore, the general wave equation (Eq. 1) can be rewritten in its one-dimensional form as reported in Eq. 3, where u is the displacement in the x direction and f is the force applied in the same direction.

$$u_{tt} = c_0^2 \frac{\partial}{\partial x}\left(\gamma(x)\frac{\partial u}{\partial x}\right) + \frac{f}{\rho} \quad (3)$$

1.2 Workflow

To solve the inversion problem for the wave equation and, thus, to perform damage identification, this work relies on Physics-Informed Neural Networks (PINN). In this framework, neural networks adapt data to the governing laws of physics of the system of interest. This is achieved by incorporating the equations describing the underlying physical phenomena as constraints, e.g., loss function, during the neural network training process. PINNs are advantageous for efficiently solving partial differential equations, modelling complex systems, and adapting to various data types [13] [14] [15] [16].

The first step is to develop tools able to solve the wave equation, with the aim of being implemented in the PINN framework. For brevity, only the procedure used to realise the finite difference solver for the mono-dimensional wave equation of Eq. 3 is shown.

The domain selected is a one-dimensional string of length L_x with the edges fully constrained and, thus, the displacement u at those points is set to zero. The wave equation is then solved in the finite difference framework using the following stencils for the partial differential equation (Eq. 4), and boundary (Eq. 5) and initial (Eq. 6) conditions:

$$u_i^{n+1} = 2u_i^n - u_i^{n-1} + c^2 \frac{dt^2}{2dx^2}[(\gamma_i + \gamma_{i+1})(u_{i+1}^n - u_i^n)] + \\ -c^2 \frac{dt^2}{2dx^2}[(\gamma_i + \gamma_{i-1})(u_i^n - u_{i-1}^n)] + \frac{dt^2}{\rho} f_i^n) \quad (4)$$

$$BC: u_0^n = 0;\ u_{N_x}^n = 0 \quad (5)$$

$$IC: u_i^0 = 0;\ \dot{u}_i^0 = 0 \quad (6)$$

where i is the index for the space position node and can assume values between 0 and N_x, while n is the index for time, varying between 0 and N_t. Consider that $N_t + 1$ is the number of time nodes and $N_x + 1$ is the number of spatial nodes of the grid, consequently dx and dt are defined as the step in space and time, respectively in Eq. 7 and in Eq. 8 where L_x is the length of the domain in x direction, while L_t is the end time of the simulation.

$$\mathrm{dx} = \frac{\mathrm{L_x}}{N_x} \quad (7)$$

$$\mathrm{dt} = \frac{L_t}{N_t} \quad (8)$$

Consider that the mono-dimensional wave equation is too simple to model Lamb wave behaviour, hence during thesis work a more complex solver has been developed for the two-dimensional case study. The solvers have been validated using the Abaqus software package.

1.3 Physics-Informed Framework Definition

The two methods developed make use of a neural network that predicts the distribution of the material on the domain, but they differ in how the loss function is defined. The prediction of material distribution is the focus of the two PINN-based methods. For the networks, the spatial position is the input, and the output is the material distribution $\gamma(x)$.
The first approach, namely the Method 1, a neural network is used to solve the inverse problem based on the measured displacement u_m [19], therefore, predicting the material properties distribution γ. The loss function is the residual of the partial differential equation. The alternative approach, called Method 2, couples a PINN with a numerical solver and is developed starting from the work presented in [18], adapting the latter to deal with Lamb waves. Such a method is selected due to the reduction in complexity of the optimization process since this method relies on a finite difference solver that computes the wave field u using the material distribution γ predicted from the PINN. Therefore, the partial differential equation is always satisfied, and the loss function is calculated as the difference between the measured displacement u_m and the predicted one. A schematic of these approaches is given in **Fig. 1(a)** for Method 1 and in **Fig. 1(b)** for Method 2.

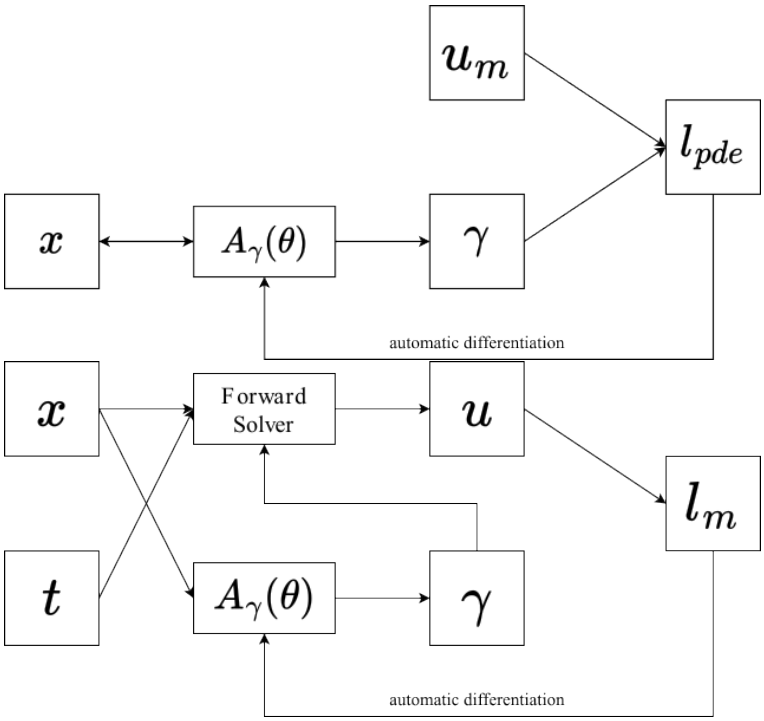

(a)

(b)

Fig. 1. Schematics of (a) Method 1 and (b) Method 2, e.g., physics-informed method coupled with finite difference solver.

2. Case studies

In this section, the two case studies analysed are described. The first one is a one-dimensional non-homogeneous clamped-clamped string, while the second one is a plate section subjected to plain strain and constrained with clamps at both ends. The first case study is used to compare the two methods presented in Section 1.3 Physics-Informed Framework Definition. Instead, only the Method 2 is tested with the second case study.

2.1 1D Case Study: String

The simulation of a wave in a one-dimensional domain is comparably simple to propagating Lamb waves in a plate and thus it makes the one-dimensional case a perfect environment to compare the two methods.

An aluminium string clamped at both ends is considered, with a length of $L_x = 10\ cm$. A force is applied in the middle using a sine wave modulated with a Hanning window with a specified number of cycles, $n_{cycles} = 3$, to reproduce the lamb wave excitation. There are 9 sensors, equally spaced along the string, and no sensor is placed on the clamped ends as shown in **Fig. 2**. A 1 cm length damage, represented by a $\gamma = 0.5$, is present in the string and is centred at 7 cm from the left end of the string.

The neural network selected is an FFNN for both methods, with x as input and γ as output, it has 4 hidden layers of 5, 10, 10, and 5 neurons per layer. The excitation force frequency is set to 25 kHz for Method 1 for numerical stability and to 300 kHz for Method 2.

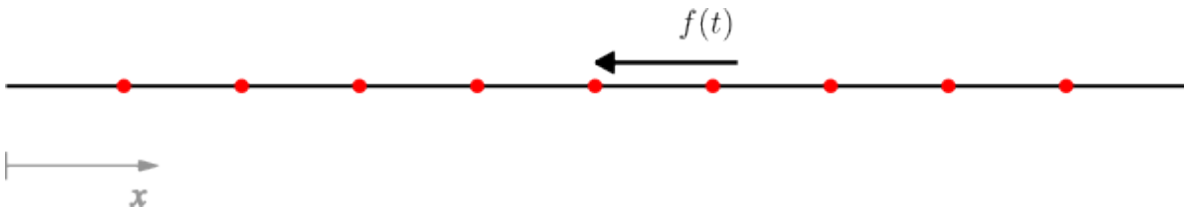

Fig. 2. Mono-dimensional case study: the red dots represent the sensor placement while the arrow is the excitation force, which is applied in the centre of the string.

2.2 2D Case Study: Plate Section

Method 2 is tested on a two-dimensional case study to correctly model Lamb waves, which is not feasible in the mono-dimensional model.

The domain selected is a plate section with two sides clamped and the other two free to move, the two dimensions are the thickness and length of the plate, the other dimension is not considered due to the plane strain condition. The plate section is made of aluminium and has the following dimensions $5 \times 5 \times 0.1\ cm$. The excitation force is placed in the middle with frequency $f = 400\ kHz$ with a configuration that excites the A0 mode. Four equally spaced sensors are placed on the upper surface and no sensor is placed at the clamped sides as represented in **Fig. 3**. The neural network selected is the same as the one described in the previous case. The material distribution is considered constant along the thickness, and damage is simulated by imposing $\gamma = 0.5$ for $x \in [3; 3.75]$.

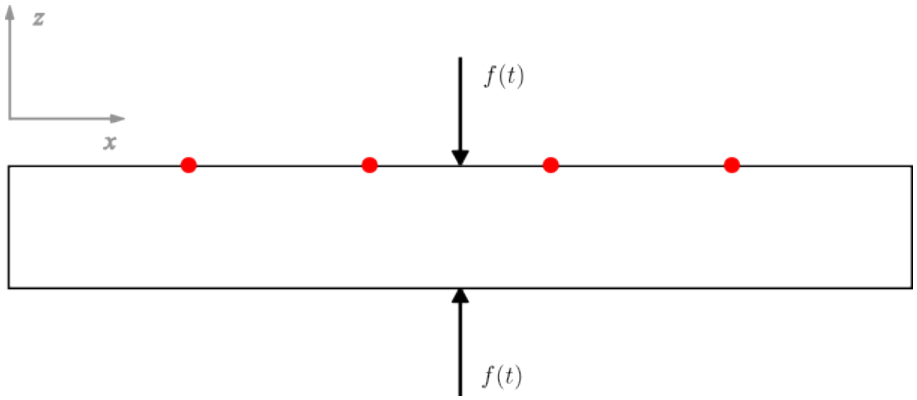

Fig. 3. Bi-dimensional case study: the red dots represent the sensor placement while the arrows are the excitation forces, applied in the centre of the plate section.

3. Results and discussion

The results of the two methods presented in Section 1.3 Physics-Informed Framework Definition, namely Method 1 and Method 2, for the two case studies described in Section 2. Case studies.

Starting with the 1D case study, **Fig. 4** shows the results of (a) Method 1 and (b) Method 2. The methods proved to be sensitive to the presence of the damage by showing a variation of the estimated material properties distribution. However, it can be noted that Method 2 outperforms Method 1 in terms of accuracy by closely following the actual γ, represented in orange, for both damage position and quantification of the loss of the material properties.

However, the increase in computational cost due to resorting to the finite difference solver at each iteration of the training process is not negligible: Method 1 completed training

in 500 s, while Method 2 needed 2000 s to achieve convergence. Thus, the improved accuracy comes at the cost of having a four times higher computational cost.

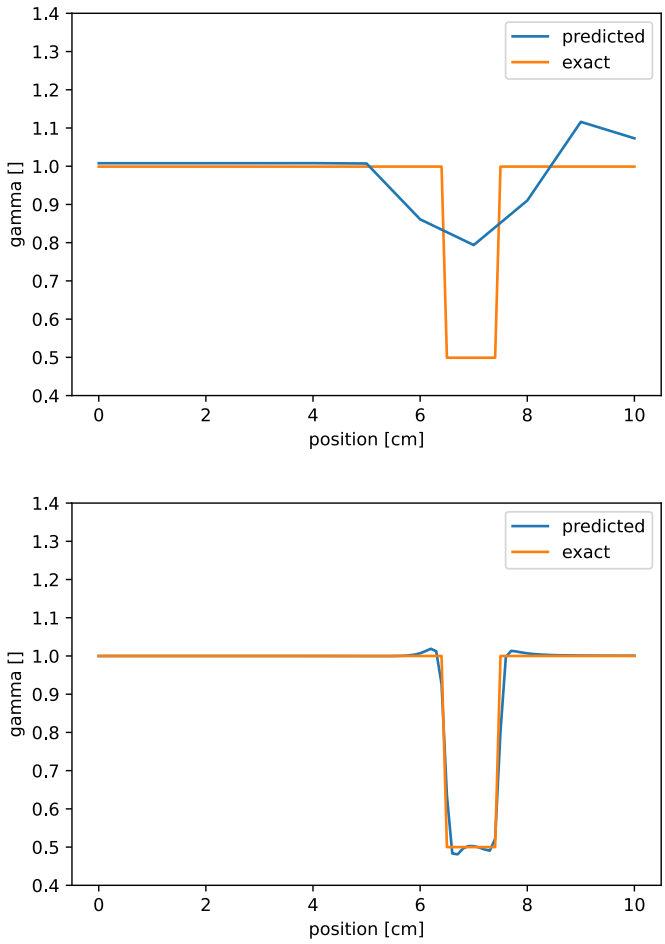

Fig. 4. Prediction of material properties distribution for (a) Method 1 and (b) Method 2 for the mono-dimensional case study.

Eventually, only the second method, e.g., Method 2, is applied in the 2D case study thanks to its proven higher accuracy with respect to the other method. **Fig. 5** shows the prediction of the proposed method, represented in blue, against the actual γ distribution, in orange. As for the mono-dimensional case study, Method 2 proves to be reliable since it can predict the reduction in material properties and the extent of the damage. Even in this case, the great flaw of this method is the computational time since the increased complexity of the finite difference solver, which is due to the increased dimensionality of the problem, raises the training time to 20000 s (which is ten times higher than for the 1D case).

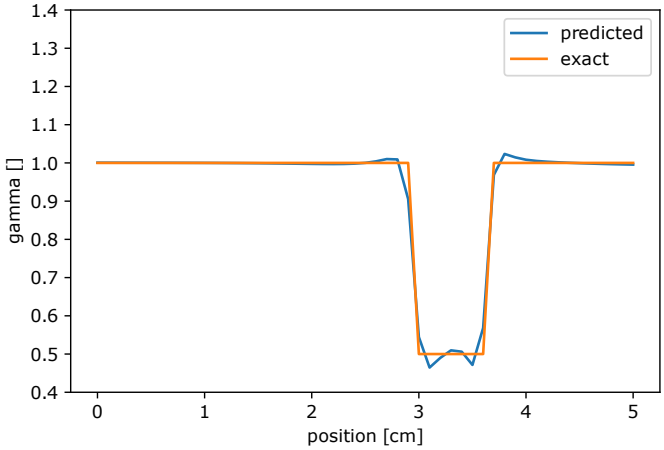

Fig. 5. Prediction of the material properties for Method 2 in the bi-dimensional case study.

To conclude, this work proves that Method 2 can guarantee higher performances with respect to Method 1, with the drawback of a significantly increased computational cost. The training time increases noticeably with the increased dimensionality of the problem, questioning the application of this method for more complex case studies. However, the high accuracy of this approach justifies the efforts for future improvements towards a reduction of the computational effort required by this method.

4. Conclusion

In this study, two physics-informed machine learning methods for damage detection are presented. Specifically, the methods are designed for thin-walled structures and exploit Lamb waves without relying on feature extraction. The methods exploit a Physics-Informed Neural Network (PINN) for the prediction of the material properties distribution of the component under analysis.

The first method, namely Method 1, uses the measured displacements to predict the material properties distribution by minimising the residual of the partial differential equation governing Lamb wave propagation. The other method, e.g., Method 2, exploits a finite difference solver to obtain the displacement field based on the estimation of the distribution of the material properties, which is optimised based on the minimisation of the error between the measured displacement and the one obtained with the solver.

Two case studies were analysed: a 1D and a 2D case study. In the mono-dimensional case, both methods effectively detected the damage location in a clamped-clamped string. However, the first method had limitations in accurately quantifying material properties in the damaged region and suffered from numerical stability problems. The second method overcame these limitations but had increased computational demands by about 4 times.

Regarding the two-dimensional case, only the second method was tested on a plate under plane strain, demonstrating its ability to detect the damage location and evaluate wave speed changes in the damaged area at the expanses of a computational cost of 10 times the one for the 1D case study for the same method. Both the good performances and the high computational demand of Method 2 are due to the embedded finite difference solver. Therefore, it is mandatory to improve efficiency for effectively implementing this method for SHM purposes. Some options can be the use of gradient clipping methods, loss function weighting, GPU training, and GPU implementation of finite difference solvers.

As a prospective expansion, evaluating the method's capacity for damage detection using sensor data obtained from an actual plate equipped with piezoelectric sensors could enhance its assessment in a real-world context.

Eventually, this work paves the way for the application of unsupervised physics-informed machine learning in the framework of Lamb waves-based damage detection for SHM purposes.

References

[1] Y. Wang, L. Qiu, Y. Luo, R. Ding and J. F., "A piezoelectric sensor network with shared signal transmission wires for structural health monitoring of aircraft smart skin," *Mechanical Systems and Signal Processing,* 2020.

[2] R. Guan, Y. Lu, W. Duan and X. Wang, "Guided waves for damage identification in pipeline structures: A review," *Structural Control Health Monitoring,* 2017.

[3] X. Zhao, H. Gao, G. Zhang, B. Ayhan, F. Yan, C. Kwan and J. L. Rose, "Active health monitoring of an aircraft wing with embedded piezoelectric sensor/actuator network: I. Defect detection, localization and growth monitoring," *Smart Materials and Structures,* 2007.

[4] Z. Su, L. Ye and Y. Lu, "Guided Lamb waves for identification of damage in composite structures: A review," *Journal of Sound and Vibration,* 2006.

[5] I. Park, Y. Jun and U. Lee, "Lamb wave mode decomposition for structural health monitoring," *Wave Motion,* 2014.

[6] C. Wang, J. Rose and F.-K. Chang, "A synthetic time-reversal imaging method for structural health monitoring," *Smart Materials and Structures,* 2004.

[7] A. Muller, B. Robertson-Welsh, P. Gaydecki, M. Gresil and C. Soutis, "Structural Health Monitoring Using Lamb Wave Reflections and Total Focusing Method for Image Reconstruction," *Applied Composite Materials.*

[8] D. Wang, L. Ye, Y. Lu and Z. Su, "Probability of the presence of damage estimated from an active sensor network in a composite panel of multiple stiffeners," *Composites Science and Technology,* 2009.

[9] F. Gao, Y. Shao, J. Hua, L. Zeng and J. Lin, "Enhanced wavefield imaging method for impact damage detection in composite laminates via laser-generated Lamb waves," *Measurement,* 2021.

[10] C. Sbarufatti, G. Manson and K. Worden, "A numerically-enhanced machine learning approach to damage diagnosis using a Lamb wave sensing network," *Journal of Sound and Vibration,* 2014.

[11] Z. Dworakowski, K. Dragan and T. Stepinski, "Artificial neural network ensembles for fatigue damage detection in aircraft," *Journal of Intelligent Material Systems and Structures,* 2016.

[12] L. Lomazzi, M. Giglio and F. Cadini, "Towards a deep learning-based unified approach for structural damage detection, localisation and quantification," *Engineering Applications of Artificial Intelligence,* 2023.

[13] M. Raissi, P. Perdikaris and G. Karniadakis, "Physics-informed neural networks: A deep learning framework for solving forward and inverse problems involving nonlinear partial differential equations," *Journal of Computational Physics,* 2019.

[14] M. Raissi, A. Yazdani and G. Karniadakis, "Hidden fluid mechanics: Learning velocity and pressure fields from flow visualizations," *Science,* 2020.

[15] M. Raissi and G. Karniadakis, "Hidden physics models: Machine learning of nonlinear partial differential equations," *Journal of Computational Physics,* 2018.

[16] E. Haghighat, M. Raissi, A. Moure, H. Gomez and R. Juanes, “A physics-informed deep learning framework for inversion and surrogate modeling in solid mechanics,” *Computer Methods in Applied Mechanics and Engineering,* 2021.

[17] M. Rasht-Behesht, C. Huber, K. Shukla and G.-E. Karniadakis, “Physics-informed Neural Networks (PINNs) for Wave Propagation and Full Waveform Inversions,” *Journal of Geophysical Research: Solid Earth,* 2021.

[18] L. Herrmann, T. Bürchner, F. Dietrich and S. Kollmannsberger, “On the Use of Neural Networks for Full Waveform Inversion,” *Computer Methods in Applied Mechanics and Engineering,* 2023.

[19] M. Rasht-Behesht, C. Huber, K. Shukla, Karniadakis and G. Em, “Physics-Informed Neural Networks (PINNs) for Wave Propagation and Full Waveform Inversions,” *Journal of Geophysical Research: Solid Earth,* 2022.